High power dual-wavelength tunable fiber laser in linear and ring cavity configurations

H. Ahmad[1*], A. A. Latif[1], M. Z. Zulkifli[1], N. A. Awang[1], and S. W. Harun[2]

[1]*Photonics Laboratory, Department of Physics, University of Malaya, 50603 Kuala Lumpur, Malaysia*

[2]*Department of Electrical Engineering, Faculty of Engineering, University of Malaya, 50603 Kuala Lumpur, Malaysia*

[*]*Corresponding author: harith@um.edu.my*

Received May 3, 2011; accepted June 10, 2011; posted online August 30, 2011

We describe and compare the performances of two crucial configurations for a tunable dual-wavelength fiber laser, namely, the linear and ring configurations. The performances of these two cavities and the tunability in the dual-wavelength output varied from 0.8 to 11.9 nm are characterized. The ring cavity provides a better performance, achieving an average output power of 0.5 dBm, with a power fluctuation of only 1.1 dB and a signal-to-noise ratio (SNR) of 66 dB. Moreover, the ring cavity has minimal or no background amplified spontaneous emission (ASE).

OCIS codes: 060.2320, 060.2410, 060.3510.

doi: 10.3788/COL201210.010603.

Dual-wavelength tunable fiber lasers (DWTFLs) are relevant to the provision of a stable and tunable dual wavelength output that can be used in many applications, such as the study of high-bit-rate soliton pulses[1], differential absorption measurement of trace gases[2], photonic generation of microwave carriers[3], and microwave photonic filters[4].

Initial research into the development of dual-wavelength fiber lasers has been limited by the inability to generate a high power lasing output. This limitation was caused by the effect of mode competition between the closely spaced wavelengths; resulting in the domination of the longer wavelength over the shorter wavelength. The mode competition itself is largely caused by the homogenous broadening effect in erbium-doped fibers (EDFs), which are normally used as the gain media for fiber-based dual-wavelength sources. To overcome the effect of the homogenous broadening in EDF-based dual-wavelength fiber laser sources, various methods have been proposed, including the cooling of the EDF in liquid nitrogen[5,6] by using elliptical EDFs[7] or by incorporating polarization maintaining fiber Bragg gratings (FBGs) for wavelength selection[8], utilizing frequency shifter in the cavity[9], and many other methods[10−13].

The key ability which is sought after in the development of a DWFTL is repeatability. Generally, multi-wavelength output generated using FBGs as filters to select specific wavelengths provide tunabilty by adjusting the strain or compression that the FBG contends with because of the repeatability issue. The reason is the difficulty to revert to the original position to produce the previous wavelength once the FBG has been modified to select a new wavelength. This problem can be overcome using a filter mechanism with a series of pre-determined wavelengths, such as an arrayed waveguide grating (AWG), as proposed in this letter.

In addition, the cavity configuration plays an important role in the generation of a high-powered output with a good signal-to-noise ratio (SNR). Numerous configurations have been proposed to generate DWFLs, such as linear cavities[14,15], ring cavities[16,17], and sigma cavity configuration[18]. This is in line with the growing research interest in the generation of high-powered DWFLs for applications such as wavelength conversion using four wave mixing (FWM)[19], generation of microwave signals[20], and generation of terahertz waves[21].

We propose the use of AWG as a tuning element because of its repeatability and also compare the two main configurations of DWTFLs, namely, the linear and ring configurations, to determine which can provide a better SNR performance.

Figure 1(a) shows the experimental setup for the linear cavity DWTFL, whereas Fig. 1(b) shows the ring configuration. The linear cavity configuration, as shown in Fig. 1(a), consists of a 5-m MetroGain (fibrecore) erbium-doped fiber with absorption coefficients of 980 and 1 550 nm at 11 and at approximately 13 dB/m, respectively. The length is chosen to meet the requirement of the pumping power of the 980-nm laser diode operating at 110 mW. The EDF is subsequently connected to a 980/1 550-nm wavelength division multiplexer (WDM). The MetroGain EDF acts both as a source for the amplified spontaneous emission (ASE) and as an amplifying medium for the DWTFL. The output ASE will travel in both directions, and the ASE on the right-hand side will be sliced by the 1×16 AWG with an interchannel spacing of 100 GHz (0.8 nm).

To generate the dual wavelength output, any two channels of the AWG can be combined into a broad-band fiber Bragg grating (BB-FBG) that also acts as a "mirror" on the right-hand side of the experimental setup. The ASE will be sliced into 16 different wavelengths, ranging from 1 536.7 (channel 1) to 1 548.6 nm (channel 16). Channel 1 and channel 16 can be connected to the input ports of the BB-FBG that will subsequently reflect these two wavelengths back into the AWG. The broadband reflection spectrum is shown in Fig. 1(c). The tunable wavelength range is approximately 11.9 nm.

Consequently, the combined output will travel to the 5-m EDF for amplification and will be emitted at the 1 550-nm port of the WDM toward port 2 of the optical

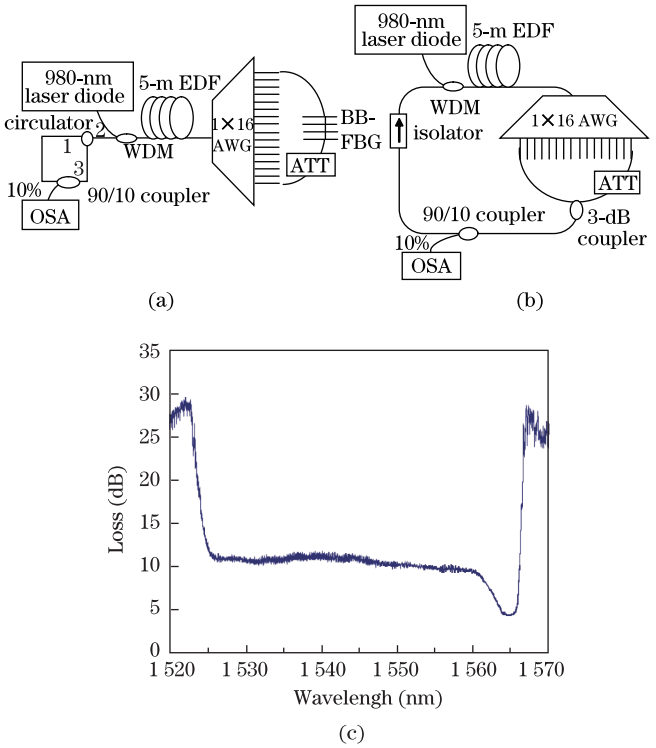

Fig. 1. (a) Linear cavity configu-ration; (b) ring cavity configuration; and (c) the BB-FBG transmission spectrum with the region of loss (dB) against wavelength, which indicates the reflection.

circulator (OC). Port 2 is connected to port 3 which facilitates the travel of the dual-wavelength output toward the 90:10 couplers with the 10% port connected to the optical spectrum analyzer (OSA). The dual wavelength will continue to travel to port 1 and will be emitted to port 2 again. This serves as the signal for the wavelength to travel to the amplifying medium for further amplification and to move onwards to the 1×16 AWG, where the whole process repeats until two lasing wavelengths of the desired power are obtained.

The tunability of these two wavelengths is accomplished by proper selection of the combinations of the channels. Erbium-doped fiber amplifiers (EDFA) exhibit homogenous broadening characteristic. Thus, mode competition can occur. The probability of the longer wavelength to lase is higher than that of the shorter wavelength.

An optical attenuator (ATT) is placed at the longer wavelength output to balance the dual wavelength output power (known as the cavity loss control method) and to create two lasing wavelengths of equal power. A similar approach is implemented on the ring configuration, as shown in Fig. 1(b).

In the ring configuration, reflecting "mirrors" are not required. Instead, the ASE generated on the right hand side of the EDF travels to the 1×16 AWG, where it will be sliced into 16 different wavelengths (channels), similar to the case of the linear cavity. For dual-wavelength output, two of the channels can be combined using a 3-dB fused coupler, which is subsequently connected to a 90:10 fused coupler in the ring cavity. Similar to the linear cavity configuration, the 10% port is connected to an OSA, whereas the 90% port is connected to an isolator to ensure unidirectional and onward travel to the 1 550-nm port of the WDM.

The common port of the WDM is connected to the EDF, which provides amplification and completes the ring cavity. Similar to the linear cavity, an attenuator is placed at the longer wavelength channel. The reason is similar as that of the previous case.

Both configurations are analyzed for their output spectra, output power, SNR, and stability to determine which of the two designs can provide the higher output power with the better SNR. The largest channel spacing available in the current experiment is 11.9 nm (channels 1 and 16), and the narrowest spacing is 0.8 nm (channels 8 and 9). These are not restricted to these channels; because various channel pair configurations can be created to provide nearly continuous channel spacing.

Figure 2 shows the spectra of the DWTFL for the linear and ring cavity configurations, whereas Fig. 2(a) presents the dual wavelength output taken in pairs from the largest to the smallest channel spacing, i.e., channels 1 and 16 (the largest), channels 2 and 15, and so on until channels 8 and 9 (the smallest), which are superimposed on the same trace. The peaks ride on the ASE background where the floor is approximately –45 dBm. The inset indicates the ASE spectra of the 5-m MetroGain fiber.

The maximum power of the dual wavelength output is approximately 0 dBm with a 3-dB bandwidth of approximately 0.025 nm for each channel. For the ring cavity, the maximum power of the dual wavelength

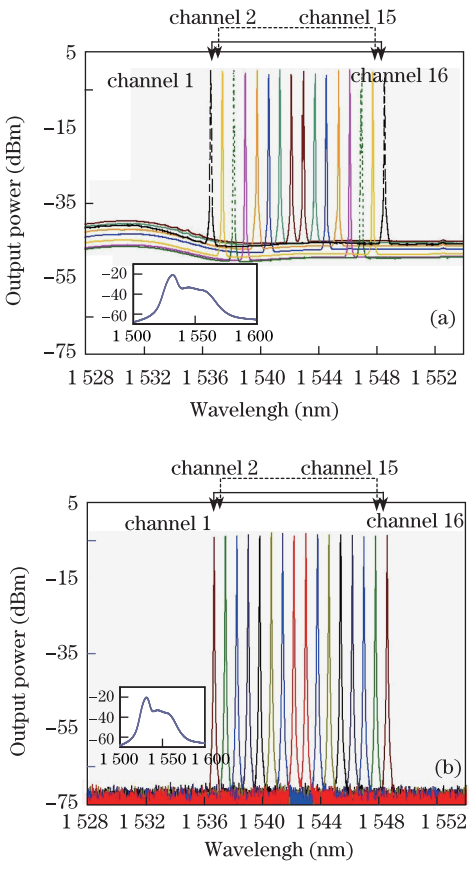

Fig. 2. DWFL spectra obtained for the (a) linear configuration; (b) ring configuration. Inset shows the ASE spectra of the 5-m MetroGain EDF.

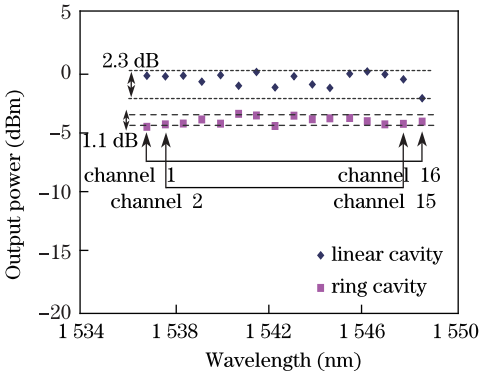

Fig. 3. DWFL output power for the ring and linear cavity configurations.

output is approximately –5 dBm. The ring cavity has a constant value throughout the process of obtaining different dual wavelength pairs. As shown in the graph, the dual wavelength pairs do not ride onto the ASE spectrum, thus producing a better SNR. The tunability of the wavelength spacing can be determined using various output channel combinations in addition to the pair scheme proposed in this letter.

The absence of the ASE background in the ring cavity is largely due to the filtering process of the cavity. In Fig. 1, the output ASE of the 5-m EDF directly travels to the 1×16 AWG that is consequently split into the various wavelengths without any ASE background. These wavelength pairs travel into the ring cavity and back to the AWG and undergo the same splitting process without having the ASE background. This is not the case with the linear cavity, where the reflected output of the 16 channels from the AWG undergoes amplification in the 5-m EDF prior to its travel toward the OC port 2. At this instance, the output consists of the multiple channels riding on top of the background ASE, which is subsequently tapped out at the 90:10 coupler.

The output powers are measured for different pair combinations, as shown in Fig. 3. The wavelengths of the pair are given as the abscissa of the graph and the ordinate is the output power. In Fig. 3, the linear cavity has an average power of approximately 0 dBm with a power variation of 2.3 dB. In the case of the ring cavity, the average power is approximately –5 dBm with a power variation of 1.1 dB. Although the linear cavity has a higher output power compared with the ring cavity, it fares poorly in terms of the SNR, as shown in Fig. 4. The slight variation in the power output in Fig. 3 can be further improved by properly cleaning the port channels of the AWG.

In Fig. 4, the SNR of the ring cavity is superior to that of the linear cavity, with an average SNR value of 66 dB compared with the value of 44 dB for the linear cavity. The SNR variation between the pair channels is approximately 2.5 dB for the ring cavity, whereas for the linear cavity, the variation is approximately 10.7 dB. This implies that the output power of the dual-wavelength output from the ring cavity is more consistent compared with the various combinations of the pair channels. In the linear cavity, the large variation of the SNR in the pair channels makes it unsuitable for applications that require a tunable dual-wavelength output with constant power. Based on this measurement, the ring cavity is an important source for a dual-wavelength with a stable and constant power.

The other important parameter in characterizing the dual-wavelength source is the stability measurement of the output power against time. This is shown in Fig. 5 for two extreme cases; one with the widest spacing (channels 1 and 16) and the second with the narrowest spacing (channels 8 and 9), as shown in Figs. 5(a) and (b), respectively. The fluctuations of the linear and the ring cavity have almost similar patterns, with variations of 1.61 and 1.22 dB, respectively, for channel 1. As for channel 16, the variation is 1.61 dB for the linear configuration, whereas the ring cavity configuration shows a variation of 1.69 dB.

Figure 5(b) shows the variation for channels 8 and 9, which are the narrowest channel spacings for the dual-wavelength laser output, with variations of 1.65

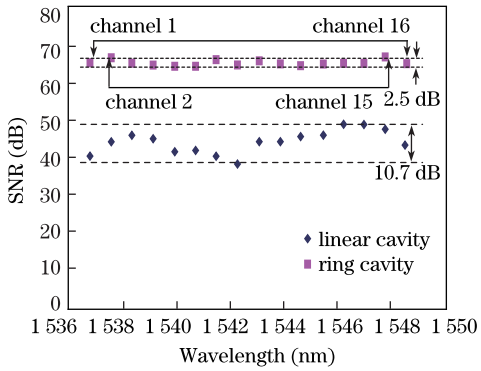

Fig. 4. SNR of DWFL output for the ring and linear cavity configurations.

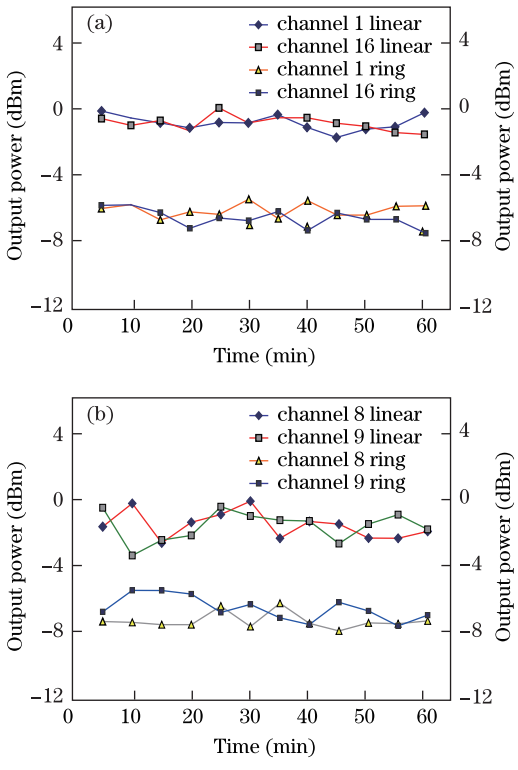

Fig. 5. Stability of the DWFL for the ring cavity and linear cavity configurations for (a) the widest spacing (channels 1 and 16) and (b) the narrowest spacing (channels 8 and 9).

and 2.49 dB, as well as 2.12 and 2.91 dB, for the ring and linear cavity configurations, respectively. Although there are slight variations in the output power stability, this can be further improved by refining the attenuation, minimizing the insertion losses, and properly cleaning the connectors.

For practical applications of tunable dual-wavelength fiber lasers, the ring cavity configuration is the best choice because it can provide a constant output power for various wavelength combinations.

In conclusion, we describe and compare the performance of two important configurations, namely, the linear and ring cavity configurations, for tunable dual-wavelength output fiber lasers. The tunability can vary from 0.8 to a maximum of 11.9 nm by selecting the various output channels from the AWG. The performance of the ring cavity is superior to that of the linear cavity, achieving a power variation of only 1.1 dB and average output power of –5 dBm. Although the linear cavity has a higher average output power of 0 dBm, the power variation between paired channels is large, with a value of 2.3 dB. Another advantage of the ring cavity is the higher SNR of 66 dB, with a fluctuation of only 2.5 dB compared with the linear cavity SNR of 44 dB, with a higher fluctuation of 10.7 dB. Therefore, the ring cavity is a suitable candidate as a tunable dual-wavelength fiber laser source.

References

1. M. Tadakuma, O. Aso, and S. Namiki, in *Proceedings of OFC′*2000 178 (2000).
2. A. J. Ruggiero, M. W. Bowers, and R. A. Young, in *Proceedings of CLEO' 99* 523 (1999).
3. L. Xia, P. Shum, and T. H. Cheng, Appl. Phys. B **86,** 61 (2007).
4. D. Liu, N. Q. Ngo, G. Ning, P. Shum, and S. C. Tjin, Opt. Commun. **266,** 240 (2006).
5. S. Yamashita and K. Hotate, IEEE Photon. Technol. Lett. **32,** 1298 (1996).
6. N. Park and P. F. Wysoncki, IEEE Photon. Technol. Lett. **8,** 1459 (1996).
7. G. Das and J. W. Y. Lit, IEEE Photon. Technol. Lett. **14,** 606 (2002).
8. S. Feng, O. Xu, S. Lu, T. Ning, and S. Jian, Opt. Commun. **282,** 825 (2009).
9. A. Bellemare, M. Karasek, M. Rochette, S. L. Rochelle, and M. Tetu, J. Lightwave Technol. **18,** 825 (2000).
10. J. Sun, Y. Dai, X. Feng, Y. Zhang, and S. Xie, IEEE Photon. Technol. Lett. **18,** 2587 (2006).
11. M. P. Fok and C. Shu, Opt. Express **15,** 5925 (2007).
12. C. H. Yeh, C. W. Chow, F. Y. Shih, C. H. Wang, Y. F. Wu, and S. Chi, IEEE Photon. Technol. Lett. **21** (2009).
13. C. H. Yeh, Opt. Express **15,** 13844 (2007).
14. D. Liu, N. Q. Ngo, X. Y. Dong, S. C. Tjin, and P. Shum, Appl. Phys. B **81,** 807 (2005).
15. X. He, X. Fang, C. Liao, D. N. Wang, and J. Sun, Opt. Express **17,** 21773 (2009).
16. J. Nilsson, Y. W. Lee, and S. J. Kim, IEEE Photon. Technol. Lett. **8,** 1630 (1996).
17. X. Chen, Z. Deng, and J. Yao, IEEE Transact. on Microwave Theory and Techniques **54,** 804 (2006).
18. S. Pan and J. Yao, Opt. Express **17,** 12167 (2009).
19. D. Z. Hsu, S. L. Lee, P. M. Gong, Y. M. Lin, S. S. W. Lee, and M. C. Yuang, IEEE Photonics Tech. Lett. **16,** 1903 (2004).
20. Y. Yao, X. Chen, Y. Dai, and S. Xie, IEEE Photon. Technol. Lett. **18,** 187 (2006).
21. I. Park, I. Fisher, and W. Elsaber, in *Proceedings of CLEO/ Europe'2003* (2003).